Ultrafast Dynamics of 1-Ethynylpyrene-Modified RNA: A Photophysical Probe of Intercalation

ARTICLE *in* THE JOURNAL OF PHYSICAL CHEMISTRY B · SEPTEMBER 2010

Impact Factor: 3.3 · DOI: 10.1021/jp103176q · Source: PubMed

4 AUTHORS, INCLUDING:

Joachim W Engels
Goethe-Universität Frankfurt am Main
300 PUBLICATIONS **4,446** CITATIONS

SEE PROFILE

Josef Wachtveitl
Goethe-Universität Frankfurt am Main
180 PUBLICATIONS **3,740** CITATIONS

SEE PROFILE

Ultrafast Dynamics of 1-Ethynylpyrene-Modified RNA: A Photophysical Probe of Intercalation

Ute Förster,[†] Christian Grünewald,[‡] Joachim W. Engels,[‡] and Josef Wachtveitl*[,†]

Institute of Biophysics and Institute of Physical and Theoretical Chemistry, Goethe-University Frankfurt, Max-von-Laue-Str. 1, 60438 Frankfurt, Germany, and Institute for Organic Chemistry and Chemical Biology, Goethe-University Frankfurt, Max-von-Laue-Str. 7, 60439 Frankfurt, Germany

Received: April 8, 2010; Revised Manuscript Received: July 9, 2010

The photophysics of pyrene attached to an adenine base within RNA single strands and duplexes is examined with respect to the position of the pyrene within the strand and the number of pyrenes attached to one duplex. Compounds with pyrenes intercalating sequence specifically are examined, as well as a doubly modified compound, where the two pyrenes are located close enough to each other for significant excimer interaction. Femtosecond transient absorption measurements and time correlated single photon counting measurements allow a thorough examination of the local influences on the pyrene photophysics. Our results suggest that optical excitation establishes an equilibration between two molecular states of different spectroscopic properties and lifetimes that are coupled only via the excited state as a gateway. One of them is a neutral pyrene−adenine excited state, S*, while the second one is connected to an excited charge transfer state, S^*_{CT}. In all compounds, an ultrafast sub-ps decay from a higher excited state into the lowest excited state S* occurs, and an excited charge transfer species S^*_{CT} is formed within picoseconds. The fluorescence behavior of the pyrene-modified adenine, however, is strongly dependent on RNA conformation. Both S* and S^*_{CT} states are fluorescent, and decay within hundreds of picoseconds and ∼2 ns, respectively. The ratio between S* and S^*_{CT} fluorescence depends strongly on pyrene intercalation, and it is found that the S* state is quenched selectively upon intercalation of the pyrene into RNA. The doubly modified duplex exhibits an additional fluorescent state with a lifetime of 18.7 ns, which is associated with the pyrene excimer state. This state coexists with a significant population of the pyrene monomer, since the characteristic features of the latter can still be observed. Formation of the excimer occurs on femtosecond time scales. The pyrene label thus provides a sensitive tool to monitor the local structural dynamics of RNA with the chromophore acting as a molecular beacon.

Introduction

Fluorescent molecules have proven useful in a wide variety of biomolecular assays both *in vivo* and *in vitro*.[1,2] They are established over the whole visible spectral range and can be applied site-specifically.[3] Fluorescence is generally highly dependent on environmental factors[4] and is therefore a well suited parameter for molecular properties of the fluorophore and its direct surroundings. Additionally, the sensitivity of the detection level reaches down to single photon events.

Pyrene and its derivatives are among the most prominent fluorescent labels, especially in the context of nucleic acids. The high sensitivity of pyrene to solvent effects[5−8] and its capability to form excited state complexes both homogeneously[9] and heterogeneously[10,11] has opened up many possibilities in the fields of RNA recognition,[12,13] electron injection,[14,15] bioengineering,[16,17] structure stabilization,[18] structure determination,[19−21] as well as nucleobase photophysics.[22−25] The photophysics of the pyrene or pyrene derivatives is extremely sensitive to the extension of the pyrene aromatic system.[26−28] Therefore, if pyrene and the corresponding base are closely connected, strong interactions between the dye and the base are to be expected. Presently, pyrene residues are attached to the 8-position of purines, the 5-position of pyrimidines, or the sugar. In contrast, we attached the pyrene to the 2-position of a purine (adenosine) for our investigation.

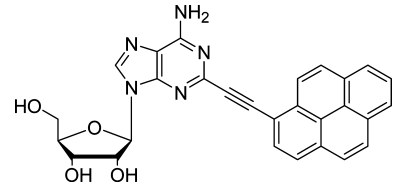

Figure 1. Chemical structure of the parent 2-(1-ethynylpyrene)-adenosine (PyrA).

In a previous study, we exploited 2-(1-ethynylpyrene)-adenosine (PyrA, Figure 1) as a general RNA folding probe.[29] We recently reported a sequence dependence of the intercalation of this label,[30] where we could distinguish between duplexes with intercalated pyrene and duplexes with the pyrene located outside of the double strand via temperature dependent pyrene fluorescence. In the same study, we tested the suitability of excimers as local probes for RNA dynamics. The photophysics of the 2-(1-ethynylpyrene)-adenosine in methanol provides clear evidence for the formation of a charge transfer state and a dual fluorescence decay of the excited state.[31]

We now aim to investigate the connection between of the above-mentioned structural differences and the photophysics of the PyrA label. We thus use a combination of femtosecond transient absorption spectroscopy and time correlated single photon counting to shed light on the ultrafast spectroscopic

* To whom correspondence should be addressed. Phone: 0049 69 798 29351. Fax: 0049 69 798 29709. E-mail: wveitl@theochem.uni-frankfurt.de.
[†] Institute of Biophysics and Institute of Physical and Theoretical Chemistry.
[‡] Institute for Organic Chemistry and Chemical Biology.

10.1021/jp103176q
Published on Web 08/13/2010

TABLE 1: Overview of Synthesized Compounds, Where 1 and 2 Represent the Two Complementary RNA Strands and the Letters P and X Denote the Pyrene-Modified or Unmodified Compounds, Respectively

strand	sequence	T_m
1P	5′-CUUUUCA^{Py}UUCUU-3′	
1X	5′-CUUUUCAUUCUU-3′	
2P	3′-GAAAACUA^{Py}AGAA-5′	
2X	3′-GAAAAGUAAGAA-5′	
1P2X	5′-CUUUUCA^{Py}UUCUU-3′ 3′-GAAAAGUAAGAA-5′	35.9 °C
1X2P	5′-CUUUUCAUUCUU-3′ 3′-GAAAAGUA^{Py}AGAA-5′	30.0 °C
1P2P	5′-CUUUUCA^{Py}UUCUU-3′ 3′-GAAAAGUA^{Py}AGAA-5′	45.5 °C

properties of the pyrene-modified adenine within RNA strands and thus the dynamics of the RNA itself.

Experimental Methods

Sample Preparation. Synthesis of oligonucleotides followed standard procedures using the well established ACE-Chemistry.[32] Site specific modification with 1-ethynyl-pyrene was accomplished by Sonogashira cross-coupling to an iodinated nucleobase (adenine) within the strand while still on solid support[33] exploiting the general advantages of solid-phase synthesis (high yield, ease of purification, etc.). 2-(1-Ethynylpyrenyl)-3′,5′-*O*-(tetraisopropyldisiloxano)-N^6-(*N*′,*N*′-dimethylamino-methyleno)-adenosine (a lipophilic pyrene-adenosine derivative as model compound) was also synthesized by Sonogashira cross-coupling of the protected, iodinated nucleoside and 1-ethynyl-pyrene.

As a prerequisite, first, 2-iodo-adenosine had to be synthesized starting with guanosine using literature procedures.[34−36] Subsequent conversion to the ACE-phosphoramidite and automated RNA synthesis yielded the solid-support bound oligonucleotide. This iodinated oligonucleotide was then reacted two times with 1-ethynyl-pyrene in a Pd-catalyzed Sonogashira cross-coupling reaction under exclusion of oxygen at room temperature for 3 h. After deprotection and cleavage from the solid support, the oligonucleotide was purified by anion-exchange HPLC. After desalting, the oligonucleotides were analyzed using MALDI-TOF mass spectrometry (see ref 29 for experimental details).

Two complementary strands were synthesized in modified and unmodified form and later hybridized to form the duplexes. An overview of the complexes and the terminology used can be found in Table 1 together with the melting temperatures. The single RNA strands are numbered; the suffix P indicates the attachment of pyrene, and the suffix X indicates the absence of pyrene. The specific sequence was chosen to provide good helix formation. It was found in a previous study[30] that the two duplexes 1P2X and 1X2P show significant structural differences. In 1P2X, the pyrene was at least partially intercalated into the RNA duplex, while, in 1X2P, the dye was located mostly outside of the strand.

All spectroscopic measurements of oligonucleotides were performed in phosphate buffer containing 10 mM NaH_2PO_4, 10 mM Na_2HPO_4, and 140 mM NaCl adjusted to pH 7.

Steady-State Spectroscopy. Absorption spectra were taken on a Jasco V670 (Jasco GmbH, Gross-Umstadt, Germany) absorption spectrometer using a fused silica cuvette with 1 mm optical path length. All absorption spectra were corrected for solvent absorption. Fluorescence spectra measurements were performed on a Perkin-Elmer LS 50 fluorimeter (Perkin-Elmer, Waltham, Massachusetts) at an excitation wavelength of 380 nm. The concentration was adjusted to ∼10 μM for all samples.

Vis-Pump/Vis-Probe Spectroscopy. A detailed description of the vis-pump/vis-probe spectroscopy setup has been given elsewhere.[37] In short, the source for the ultrashort laser pulses was a CLARK CPA 2001 (Clark-MXR, Dexter, MI). It provided laser pulses of a pulse energy of 800 μJ at 775 nm with a pulse duration of 170 fs. The excitation pulses of 180 μJ at 387 nm were generated by frequency doubling of the laser fundamental in a BBO crystal cut to 29.5° for optimal phase matching. Single filament supercontinuum white light pulses were generated in a CaF_2 plate and then split into two beams for probe and reference detection. Two identical 42-segment diode arrays were used for spectrally broad detection of the absorption and reference signal.

A fused silica cuvette with 1 mm optical path length was moved perpendicular to the incident beam to avoid excessive photobleaching.

UV−vis absorption spectra were taken before and after the measurement. These spectra could give assurance that the photodamage to the chromophores was low and also indicated that little degradation of the modified RNA occurred during measurement.

Time Correlated Single Photon Counting Fluorescence Spectroscopy (TCSPC). A detailed description of the combined TCSPC/upconversion setup has been given elsewhere.[31] In short, a Spectra Physics Tsunami-Spitfire-system (Newport Spectra Physics, Irvine, California) served as the fs-pulse source, yielding 100 fs pulses with a pulse energy of 1.2 mJ at 800 nm. The excitation pulses of 120 μJ at 400 nm were generated in a manner similar to the transient absorption experiment by frequency doubling of the laser fundamental. Emission was detected after spectral selection via a Jobin-Yvon D3-180 Gemini double monochromator (Horiba Jobin-Yvon, Unterhaching, Germany) by a Becker & Hickl MSA 1000 counting system (Becker & Hickl, Berlin, Germany) using a cooled single photon counting detector head PMC 100-4 (Becker & Hickl, Berlin, Germany). The time resolution of the counting card was 1 ns. Like in the absorption experiment, a fused silica cuvette with 1 mm optical path length was used and moved perpendicular to the incident beam. Fluorescence spectra were taken before and after measurement to estimate the photoinduced long-term bleach.

Data Analysis. Transient absorption measurements: Several corrections of the raw data set are necessary prior to the application of a fitting procedure to the absorption data: solvent signals have to be subtracted and the transients have to be corrected for group velocity dispersion using a procedure introduced by Kovalenko et al.,[38] which takes the temporal evolution of the coherent signal of pure buffer solution into account.

For the quantitative analysis of the absorption data, we used a kinetic model that describes the data as a sum of n exponential decays with the associated lifetimes τ_i, convoluted with the system response function. The model assumes Gaussian pump and probe pulses with a 1/e cross correlation width t_{cc}.

A Levenberg−Marquardt algorithm optimizes a number of time constants simultaneously to the whole spectrum, yielding wavelength dependent amplitudes $A_i(\lambda)$, so-called decay associated spectra (DAS) corresponding to the different time constants applied.

$$\Delta A(\lambda, t) = \sum_{i=1}^{n} A_i(\lambda) \exp\left(\frac{{t_{cc}}^2}{4\tau_i} - \frac{t}{\tau_i}\right) \cdot \frac{1}{2} \cdot \left(1 + \mathrm{erf}\left(\frac{t}{t_{cc}} - \frac{t_{cc}}{2\tau_i}\right)\right)$$

TCSPC Measurements. TCSPC measurements were corrected for stray light from the excitation beam. Then, the same global fit analysis method as described above for the transient absorption scheme was also applied for the TCSPC measurements. A cross correlation of 1.2 ns, resulting from a Gaussian fit of the instrument response function of the system, was used for deconvolution.[31]

Results and Discussion

Steady-State Characterization. Absorption spectra were taken for all five pyrene-modified compounds (Figure 2A). The spectra exhibit similar shapes including two absorption maxima of the pyrene−adenine moiety located roughly at 380 and 410 nm, respectively, and a shoulder at 360 nm. An additional shoulder associated with pyrene is located around 320 nm but is partially covered by the RNA absorption centered at 260 nm. The overall spectra are very similar to the ones of 1-ethynylpyrene linked to the 5-position of DNA bases as examined by Rist et al.[39] The shape of the pyrene absorption band is similar to that of 1-ethynylpyrene in solution;[40] however, the band is red-shifted by almost 50 nm with respect to both pyrene and 1-ethynylpyrene and spectrally broadened significantly. This leads to the conclusion that the electronic coupling of the 1-ethynylpyrene dye with the adenine base is quite strong.[31] The region between 330 and 440 nm can therefore be associated with the transition into the first allowed excited state, while the band situated around 320 nm is associated with the absorption into higher excited states.

A small red-shift can be seen in 1P2X compared to 1P; this effect however is absent in 1X2P (and the corresponding pyrene-modified single strand 2P). The ratio between the two major pyrene bands changes upon hybridization of the RNA; however, these effects have already been discussed in ref 30 and are not a subject of this study.

The pyrene absorption spectrum of the doubly modified duplex is slightly red-shifted with respect to the singly modified duplexes, indicating that a pyrene−pyrene complex is partially present already in the ground state of the compound. Such a complex would commonly lower the energies of both the ground state and the excited state. Due to the usually higher polarity of the excited state, the effect of dimerization is often more prominent in the excited state, leading to an overall red shift of the absorption band. The observation of a red-shifted absorption is in contrast to the common notion of an excimer complex, which is usually encountered in pyrenes at close proximity, where the interaction between the two pyrenes is limited to the excited state.[9] The reason for this substantial difference may be found in the fact that the two pyrenes are connected directly to the RNA and are thus fixed at a distance of roughly 4 Å. A classic excimer, on the other hand, is usually found in solution, where the mean distance of two pyrene dyes is considerably larger. As a result, in solution, even at high concentration, ground-state interaction is not seen.

Figure 2B shows the fluorescence spectra of the pyrene-modified single and double strands. The spectra were taken at equal concentrations and corrected for absorption at the excitation wavelength. They therefore represent an estimate of the relative quantum efficiency. All compounds exhibit broad, nearly featureless spectra that can be distinguished mostly by their shape and central wavelength. Compared to the 1-ethynylpyrene fluorescence, which shows a variety of characteristic bands located around 400 nm,[40] the observed fluorescence is strongly red-shifted by 50 nm, losing almost all vibrational fine structure, as already observed in several similar systems.[11,14,41,42] This strongly indicates the presence of a partial charge transfer between the pyrene and the adenine into an excited charge transfer state S^*_{CT} and the formation of intramolecular exciplexes.[15,25,26,43] The quantum efficiencies of the singly modified duplexes vary strongly. In previous studies, similar variations have been attributed to different conformations of the pyrene within the RNA.[11,41,44] Previous studies conducted in our group allowed us to conclude via temperature dependent fluorescence measurements that, in the 1P2X duplex, pyrene is intercalated into the RNA base stack, while, in 1X2P, pyrene is located outside of the double strand.[30] Intercalation into the strand leads to substantial quenching of the pyrene fluorescence due to stacking interactions,[11,44] resulting in an overall lower quantum efficiency of 1P2X compared to 1X2P.[30]

The doubly modified RNA duplex exhibits an additional fluorescence red-shift of 35 nm with respect to the singly modified duplexes. This is due to the pyrene−pyrene interaction in the excited state, which leads to excimer-like fluorescence, as observed in similar systems before.[16,29,45,46] A pyrene−pyrene ground state interaction could already be observed in the absorption spectra. The effect on the absorption spectrum, however, is relatively small compared to the 35 nm shift of the pyrene fluorescence. This leads to the conclusion that, in addition to the ground state dimer, excited state complexes are formed. The large shift of the fluorescence wavelength shows that the excited state interaction is the dominating contribution of the pyrene dimer formation.

UV−vis Transient Absorption Measurements. Figure 3 shows the time-resolved transient absorption of all five pyrene-modified compounds. The general spectral features are very similar. A broad positive absorbance change is observed between 530 nm and the red end of the spectral observation window, which can be interpreted as the excited state absorption band (ESA). It is blue-shifted by ∼20 nm in 1P2P with respect to the other compounds. As discussed above, this effect can be attributed to the presence of an exciplex-like state in the doubly modified compound.

A ground state bleach (GSB) exhibiting two maxima can be seen up to 420 nm, corresponding well to the bands of the steady-state absorption spectra. Around 450 nm, stimulated emission appears. This band is red-shifted in 1P2P with respect to the singly modified compounds, as already mentioned in the previous paragraph. Therefore, it strongly overlaps with the excited state absorption and cannot be resolved. It can be concluded from the simultaneously occurring shifts of ESA and fluorescence in 1P2P that the higher excited states are less affected by the presence of the second pyrene than the first excited state.

In all compounds, a dynamic blue shift of the ESA of about 10 nm can be observed, which occurs on the order of a few picoseconds and corresponds to a similar red-shift in the stimulated emission region. Prior to quantitative analysis, it can already be seen that all compounds exhibit a relatively long general recovery time of >1 ns, with the notable exception of 1P2X, which shows a significantly faster overall recovery. On the other hand, the temporal characteristics of 1P2P suggest a recovery time which clearly exceeds the experimental observa-

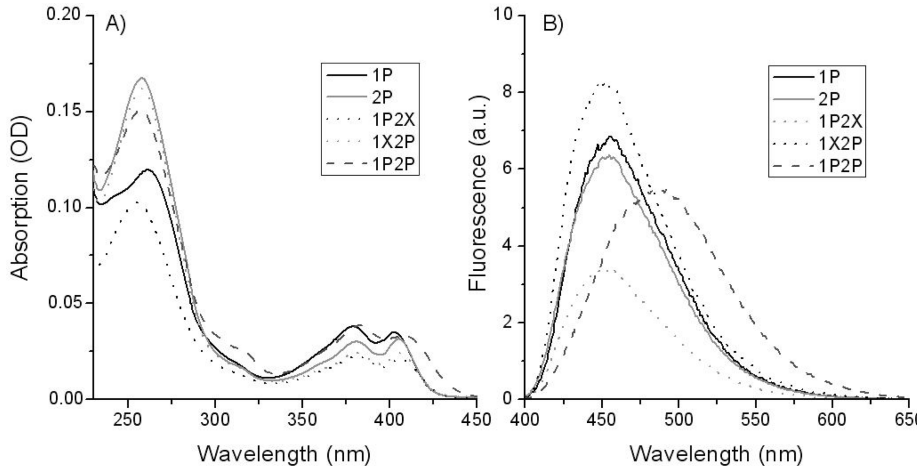

Figure 2. (A) Absorption spectra of modified single and double stranded RNA. The lowest pyrene transition ranges from 350 to 430 nm; pyrene S_0-S_n absorption is located around 300−330 nm and is significantly weaker than the lowest transition. Nucleobase absorption can be found around 260 nm. All spectra were taken at a concentration of ~10 μmol in buffer solution at room temperature. (B) Fluorescence spectra of modified single and double stranded RNA. Spectra were corrected for absorption at an excitation wavelength of 385 nm and are therefore allowing a relative estimate of the samples' quantum efficiency. All spectra were taken at a concentration of ~10 μmol in buffer solution at room temperature.

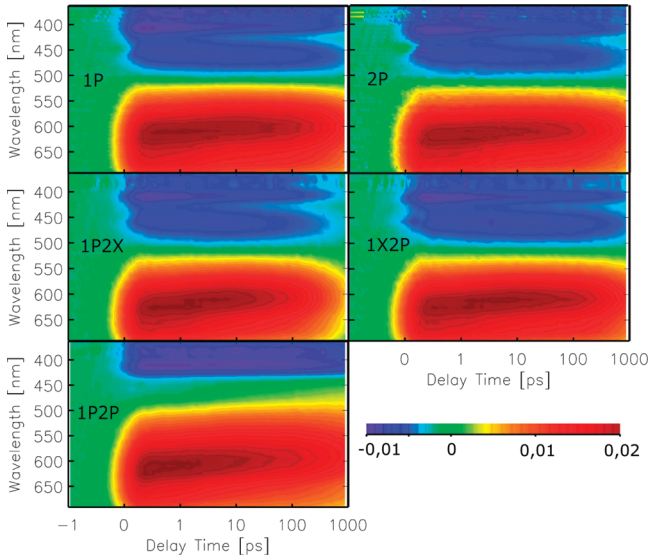

Figure 3. Transient absorption spectra of all pyrene-modified compounds. Spectra are color-coded, with red indicating positive relative absorption and blue indicating negative relative absorption. The time axis is linear up to 1 ps and logarithmic for longer delay times. All spectra were taken at a concentration of ~5−10 μmol in buffer solution at room temperature.

TABLE 2: Time Constants of Pyrene Labeled RNA Model Compounds Obtained by Global Fit Analysis of the Transient Absorption Measurements

	τ_1	τ_2	τ_3	τ_4
1P	120 fs	2.7 ps	270 ps	2 ns
2P	85 fs	2.8 ps	295 ps	2.1 ns
1P2X	114 fs	3.7 ps	350 ps	2.1 ns
1X2P	160 fs	3.6 ps	550 ps	2.4 ns
1P2P	210 fs	5 ps	275 ps	5 ns

tion window. It can already be concluded at this stage that, apart from the spectral differences between 1P2P and the singly modified compounds, the changes in the overall recovery time of the system appear to reflect most directly the structural differences of the examined compounds.

All five data sets have been analyzed by the global fit routine as described above. For each of the five pyrene-modified compounds, four time constants were required for an optimized fit and are shown in Table 2. The corresponding wavelength-dependent amplitudes (DAS) are depicted in Figure 4.

The shortest decay constant τ_1 ranges from 85 to 210 fs, and is thus in the range of the temporal resolution of the system. Its general features are also obstructed by coherent effects, especially around the excitation wavelength, due to the overlap of pump and probe pulses.[47] Nonetheless, a tentative discussion of the long wavelength range of the DAS, which shows several common features, is possible. All DAS contain a positive contribution in the red wing and a negative contribution at the blue wing of the excited state absorption. In addition to this, a positive contribution in the range of the stimulated emission can be seen for the singly modified compounds. While, as already mentioned, the DAS of τ_1 for all compounds are certainly perturbed by coherent effects (such as wavepacket motion),[47] they show some general characteristics of relaxation into the lowest level of the S* state. It is a commonly accepted feature of the photophysics of pyrene and many of its derivatives that excitation mostly occurs into the S_2 state, followed by a fast S_1 population.[26,27,48−50] However, the comparatively fast overall recovery time of the system observed in this study suggests an allowed S_1-S_0 transition, and thus the directly excited state is presumed to be the S_1 state. The deexcitation process seems to be slightly faster if the pyrene modification is located on strand 2.

For the doubly modified compound 1P2P, the DAS look slightly different. This can partially be explained by the fact that the ESA is blue-shifted for the pyrene−pyrene dimer. In addition to this, non diffusion controlled excimer formation should occur on this time scale, and is superimposed to the other processes, obscuring the dynamics of the decay into S*.

The second decay constant τ_2 ranges from 2.7 to 5 ps. It corresponds to a dynamic shift, which is visible in both the excited state absorption and the stimulated emission. A similar behavior has been observed in pyrenyl biphenyl esters,[26] 5-(1-ethynylpyrene)-uracil,[14] and the modified base used in this study,[31] and has been assigned to a charge-transfer process, forming an excited pyrene−adenine charge-transfer state (S^*_{CT}).[25] The charge-transfer process is slower in the duplexes, compared to the single strands in solution. Possibly, the π-stacking interactions within the base stack render charge transfer into the RNA slightly more unfavorable. The transition

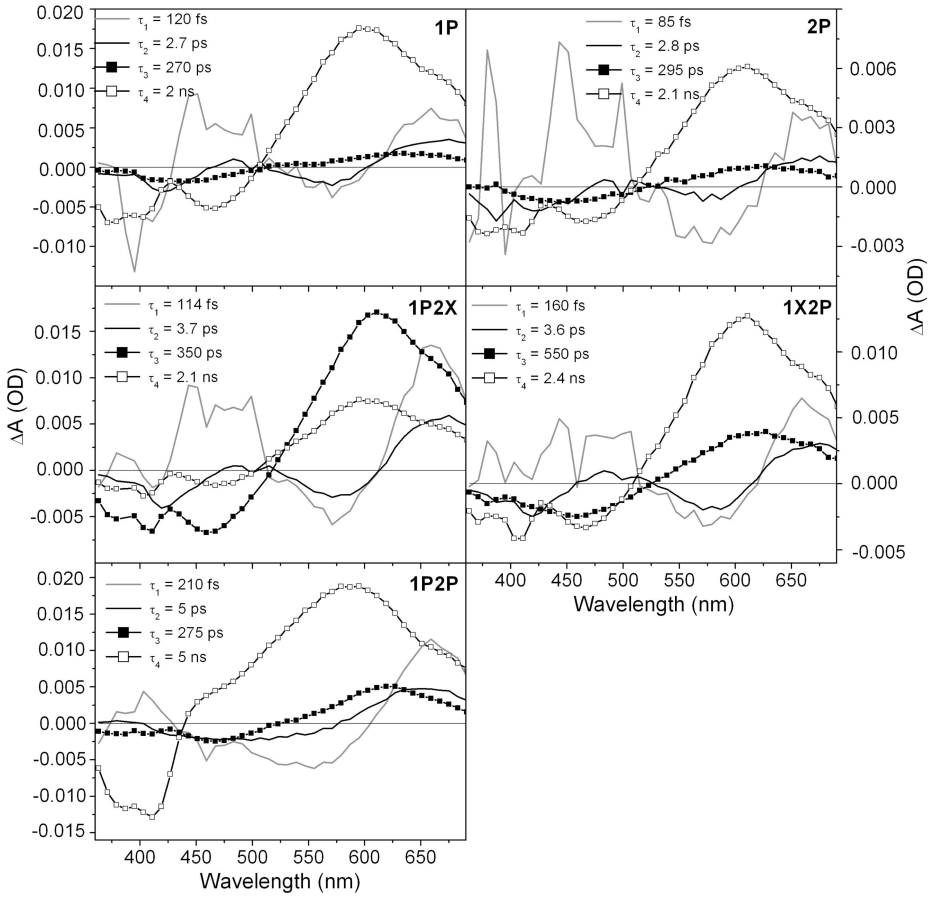

Figure 4. Decay associated spectra (DAS) for 1P, 1P2X, 1X2P, and 1P2P as obtained by a global fitting procedure. Four time constants were sufficient to describe the data in each case.

is even slower in the doubly modified duplex, where the pyrene excimer is probably less likely to transfer an electron into the base stack than the monomer.

The third and fourth decay constants τ_3 and τ_4, ranging from 270 to 550 ps and from 2 to 5 ns, respectively, both show a strong positive signal in the range of the excited state absorption, and negative signals in the stimulated emission band and in the range of the ground state absorption. The spectral characteristics can therefore be attributed to the S^*_{CT} and S* decays. Here, the largest differences between the individual compounds become evident. In the singly modified compounds, the central wavelengths of both the excited state absorption and the fluorescence differ by about 15 nm, and can thus be attributed to two different states. Since a S^*_{CT} state, which is slightly lower in energy than the S* state, is likely to be present in the compound, the lower-energy transition (τ_4) can be attributed to the fluorescence of the S^*_{CT} state, while the higher-energy transition (τ_3) corresponds to the fluorescence of the S* state. It should be noted that both fluorescence contributions are broad and featureless. While for the S^*_{CT} state this was to be expected, the featureless characteristics of the excited state fluorescence allow the conclusion that the excitation in S* is delocalized over both the pyrene and the adenine part, thus broadening the fluorescence spectrum significantly.

The ratio between the longer and shorter lifetimes varies from compound to compound. While a direct comparison of the DAS amplitudes is difficult due to the different spectral characteristics for τ_3 and τ_4, the ratio of the ESA maximum amplitudes can be used for a qualitative discussion. For the single strands, the A_3/A_4 ratio was found to be small (0.10 for 1P, 0.18 for 2P) and higher in 1X2P (0.31). However, the relation between the S^*_{CT} and S* fluorescence components is reversed in 1P2X, where the A_3/A_4 ratio is 2.2. A quantitative comparison of the fluorescence amplitudes derived from the DAS and a correlation to the samples' quantum efficiencies is not possible due to variations in the experimental conditions and the overlap of the ESA and the stimulated emission bands. However, connection of the amplitude ratios to the steady-state quantum efficiencies of the pyrene-modified RNA strands (as shown via the steady-state fluorescence spectra, and, in more detail, in ref 30) allows a qualitative discussion of the lifetime distribution. 1P2X shows a considerably smaller quantum efficiency than any of the single strands or the other singly modified duplex 1X2P. As mentioned before, the reason for this can be found in the intercalation of pyrene, and thus efficient quenching of the pyrene fluorescence.[30,44] Comparison of the A_3/A_4 ratio of 1P and 1P2X shows that the long-lived fluorescence state, which is associated with the S^*_{CT} state, is quenched selectively. The single strands in general show a smaller A_3/A_4 ratio than the duplexes. Thus, in single strands, the fluorescence of the S^*_{CT} state is generally more pronounced with respect to the S* state. This might be explained by the energy distribution along a base-paired stack, which could render fluorescence from the S^*_{CT} state more unfavorable with respect to other decay paths. The higher fluorescence quantum efficiency in 1X2P compared to its single strand 1P in solution results from a selective enhancement of the fluorescence of the S* state.

For the doubly modified compound, fluorescence lifetimes of 275 ps and 5.1 ns were found. However, the latter time constant is well beyond the experimental delay time range and

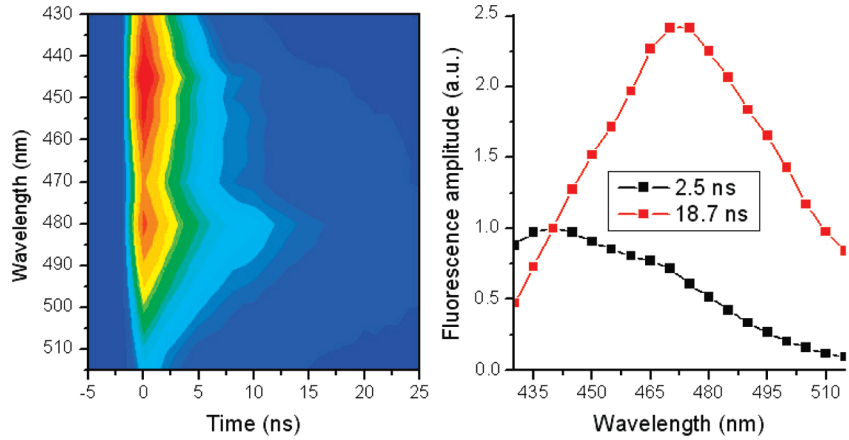

Figure 5. Left: 2-D fluorescence spectra of strand 1P2P. The spectrum is color-coded, with blue indicating no fluorescence and red indicating maximum fluorescence. Right: Global fit analysis of the measurement that shows two decay times associated with two separate spectra.

is difficult to determine directly in a pump−probe experiment. The spectral features of τ_3 are nearly identical to those of the corresponding components in the singly modified compounds. This leads to the conclusion that the S* fluorescence is not disturbed by the presence of the second pyrene but coexists with the exciplex state. A TCSPC experiment, which is better suited for this time regime, was thus carried out to further analyze the long-lived fluorescent state.

TCSPC Measurements. Figure 5 shows the TCSPC measurements on the doubly modified duplex 1P2P. It can be readily seen that, in the shorter wavelength range, the fluorescence decays significantly faster than for longer wavelengths. A global fit, carried out as described above, yields two different decay constants of 2.5 and 18.7 ns, which are spectrally well separated from one another. The decay associated spectra (Figure 5, right) underline the spectral differences of the two components. The amplitude of the smaller time constant exhibits the spectral features of the monomer pyrene S^*_{CT} fluorescence known from the singly modified compounds. The additional second component of 18.7 ns was not found in the TCSPC measurements of any of the singly modified strands or duplexes (data not shown) and can therefore be unambiguously associated with the pyrene excimer. The doubly modified compound thus exhibits three fluorescence decay times in total: 275 ps (which is not visible in the TCSPC experiment due to the time resolution of 1 ns), 2.5 ns, both being associated with the monomer complex, and 18.7 ns, associated with the pyrene excimer. The pyrene population of the doubly modified compound can therefore be divided into a monomer component, which exhibits all characteristics of the monomer photophysics, and an excimer component, which shows a significantly different behavior. The separation into these two populations occurs very early after excitation, since no mutual influences of monomer and excimer fluorescence can be observed. Another explanation might be found in the heterogeneity of the sample, thus a superposition of different populations.

Conclusions

On the basis of the structural conclusions drawn in ref 30 for the same system, we investigated the structural influences of intercalation and dimerization of pyrene attached to RNA with femtosecond pump−probe absorption spectroscopy and time correlated single photon counting. The observation of the ultrafast photodynamics of the pyrene in various positions

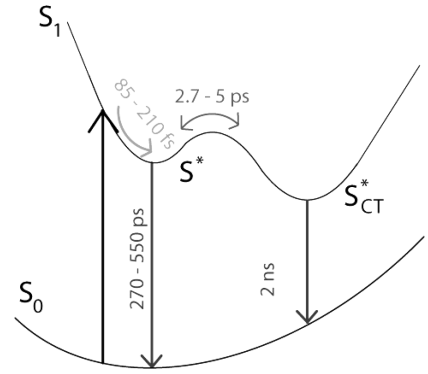

Figure 6. Reaction scheme for the singly modified RNA strands.

relative to the duplex allows us to draw conclusions on the interactions between the label and its local environment.

Examination of two singly modified duplexes—one with pyrene intercalated and the other one with pyrene located outside of the duplex—and a doubly modified compound as well as the comparison to singly modified single strands allowed us to examine the influence of various RNA surroundings on the photophysics of pyrene.

Figure 6 summarizes the conclusions for the photophysics of the singly modified RNA strands. Excitation probably occurs into a hot S_1 state, even though an excitation into a higher excited state cannot be completely excluded. Within a time frame of 85−210 fs, the system reaches the lowest excited state S*. While results in this time regime have to be interpreted carefully due to the limited time resolution of the setup, it can be stated that in the doubly modified duplex this process exhibits the longest lifetime of all compounds. Presumably, in 1P2P, the observed spectral characteristics originate not only from an ultrafast decay from a higher excited state to the S* state but also from excimer formation, which, for densely packed pyrenes, may occur on the same time scale.

From the S* state, a charge transfer state S^*_{CT} can be reached. The formation time of the charge transfer state is on the order of a few picoseconds. It is slower in duplexes, presumably due to the π-stacking between the RNA bases, and slowest in 1P2P.

From both S^*_{CT} and S* states, fluorescence into the ground state occurs. The S* state exhibits a lifetime of a few hundred picoseconds, while the decay time of the S^*_{CT} state occurs on the order of 2 ns. The ratio between the two decay

channels is dependent on the position of the pyrene within or outside the RNA strand. For intercalated pyrene, the S* state fluorescence dominates the emission behavior. This allows the conclusion that upon intercalation the S^*_{CT} state is quenched selectively, due to the greater overlap of the π-system of the excited molecule with the π-system of the surrounding bases.

In the doubly modified compound, an additional fluorescence lifetime of 18.7 ns could be detected and associated with pyrene excimer emission. It was found, however, that the ultrafast dynamics of the pyrene-base compound remains otherwise nearly unchanged, which leads to the conclusion that formation of the pyrene complex must occur from higher excited states and thus within the time resolution of the system.

Acknowledgment. The authors thank Dr. Markus Braun for helpful discussions and suggestions and the Cluster of Excellence "Macromolecular Complexes" of the University of Frankfurt for financial support.

References and Notes

(1) Valeur, B. *Molecular Fluorescence*; Wiley-VCH: Weinheim, Germany, 2002.

(2) Haugland, R. P. *Handbook of Fluorescent Probes and Research Chemicals*; Molecular Probes: Eugene, OR, 2002.

(3) Lakowizc, J. R. *Principles of Fluorescence Spectroscopy*, 2nd ed.; Springer: Berlin, 1999.

(4) Birks, J. B. *Photophysics of Aromatic Molecules*; Wiley-Interscience: London and New York, 1970.

(5) Nakajima, A. Intensity Enhancement Induced by Solute-Solvent Interaction between Pyrene and Polar-Solvents. *Spectrochim. Acta, Part A* **1982**, *38*, 693–695.

(6) Nakajima, A. Fluorescence-Spectra of Pyrene in Chlorinated Aromatic Solvents. *J. Lumin.* **1976**, *11*, 429–432.

(7) Nakajima, A. Fluorescence Lifetime of Pyrene in Different Solvents. *Bull. Chem. Soc. Jpn.* **1973**, *46*, 2602–2604.

(8) Hara, K.; Ware, W. R. Influence of Solvent Perturbation on the Radiative Transition-Probability from the B-1(Iu) State of Pyrene. *Chem. Phys.* **1980**, *51*, 61–68.

(9) Förster, T. Excimers. *Angew. Chem., Int. Ed.* **1969**, *8*, 333–343.

(10) Nakajima, A. Intensity Enhancement Caused by Complex-Formation between Pyrene and Alcohols. *Bull. Chem. Soc. Jpn.* **1983**, *56*, 929–930.

(11) Seo, Y. J.; Ryu, J. H.; Kim, B. H. Quencher-free, end-stacking oligonucleotides for probing single-base mismatches in DNA. *Org. Lett.* **2005**, *7*, 4931–4933.

(12) Okamoto, A.; Kanatani, K.; Saito, I. Pyrene-labeled base-discriminating fluorescent DNA probes for homogeneous SNP typing. *J. Am. Chem. Soc.* **2004**, *126*, 4820–4827.

(13) Mahara, A.; Iwase, R.; Sakamoto, T.; Yamaoka, T.; Yamana, K.; Murakami, A. Detection of acceptor sites for antisense oligonucleotides on native folded RNA by fluorescence spectroscopy. *Bioorg. Med. Chem.* **2003**, *11*, 2783–2790.

(14) Trifonov, A.; Raytchev, M.; Buchvarov, I.; Rist, M.; Barbaric, J.; Wagenknecht, H. A.; Fiebig, T. Ultrafast energy transfer and structural dynamics in DNA. *J. Phys. Chem. B* **2005**, *109*, 19490–19495.

(15) Wanninger-Weiss, C.; Valis, L.; Wagenknecht, H. A. Pyrene-modified guanosine as fluorescent probe for DNA modulated by charge transfer. *Bioorg. Med. Chem.* **2008**, *16*, 100–106.

(16) Nakamura, M.; Murakami, Y.; Sasa, K.; Hayashi, H.; Yamana, K. Pyrene-zipper array assembled via RNA duplex formation. *J. Am. Chem. Soc.* **2008**, *130*, 6904–6905.

(17) Maie, K.; Nakamura, M.; Yamana, K. Photocurrent responses from pyrene-modified RNA duplexes on gold surface. *Nucleic Acids Symp Ser.* **2007**, 319–320.

(18) Filichev, V. V.; Astakhova, I. V.; Malakhov, A. D.; Korshun, V. A.; Pedersen, E. B. 1-, 2-, and 4-Ethynylpyrenes in the Structure of Twisted Intercalating Nucleic Acids: Structure, Thermal Stability, and Fluorescence Relationship. *Chem.—Eur. J.* **2008**, *14*, 9968–9980.

(19) Wang, G. J.; Bobkov, G. V.; Mikhailov, S. N.; Schepers, G.; Van Aerschot, A.; Rozenski, J.; Van der Auweraer, M.; Herdewijn, P.; De Feyter, S. Detection of RNA Hybridization by Pyrene-Labeled Probes. *ChemBioChem* **2009**, *10*, 1175–1185.

(20) Silverman, S. K.; Cech, T. R. RNA tertiary folding monitored by fluorescence of covalently attached pyrene. *Biochemistry* **1999**, *38*, 14224–14237.

(21) Kawai, K.; Yoshida, H.; Takada, T.; Tojo, S.; Majima, T. Formation of pyrene dimer radical cation at the internal site of oligodeoxynucleotides. *J. Phys. Chem. B* **2004**, *108*, 13547–13550.

(22) Netzel, T. L.; Zhao, M.; Nafisi, K.; Headrick, J.; Sigman, M. S.; Eaton, B. E. Photophysics of 2′-Deoxyuridine (Du) Nucleosides Covalently Substituted with Either 1-Pyrenyl or 1-Pyrenoyl - Observation of Pyrene-to-Nucleoside Charge-Transfer Emission in 5-(1-Pyrenyl)-Du. *J. Am. Chem. Soc.* **1995**, *117*, 9119–9128.

(23) Manoharan, M.; Tivel, K. L.; Zhao, M.; Nafisi, K.; Netzel, T. L. Base-Sequence Dependence of Emission Lifetimes for DNA Oligomers and Duplexes Covalently Labeled with Pyrene - Relative Electron-Transfer Quenching Efficiencies of a-Nucleoside, G-Nucleoside, C-Nucleoside, and T-Nucleoside toward Pyrene. *J. Phys. Chem.* **1995**, *99*, 17461–17472.

(24) Amann, N.; Pandurski, E.; Fiebig, T.; Wagenknecht, H. A. A model nucleoside for electron injection into DNA: 5-pyrenyl-2 ′-deoxyribose. *Angew. Chem., Int. Ed.* **2002**, *41*, 2978–2980.

(25) Huber, R.; Fiebig, T.; Wagenknecht, H. A. Pyrene as a fluorescent probe for DNA base radicals. *Chem. Commun.* **2003**, 1878–1879.

(26) Fiebig, T.; Stock, K.; Lochbrunner, S.; Riedle, E. Femtosecond charge transfer dynamics in artificial donor/acceptor systems: Switching from adiabatic to nonadiabatic regimes by small structural changes. *Chem. Phys. Lett.* **2001**, *345*, 81–88.

(27) Pandurski, E.; Fiebig, T. Femtosecond dynamics in directly linked pyrenyl donor-acceptor systems: orbital control of optical charge transfer in the excited state. *Chem. Phys. Lett.* **2002**, *357*, 272–278.

(28) Maeda, H.; Maeda, T.; Mizuno, K.; Fujimoto, K.; Shimizu, H.; Inouye, M. Alkynylpyrenes as improved pyrene-based biomolecular probes with the advantages of high fluorescence quantum yields and long absorption/emission wavelengths. *Chem.—Eur. J.* **2006**, *12*, 824–831.

(29) Grünewald, C.; Kwon, T.; Piton, N.; Förster, U.; Wachtveitl, J.; Engels, J. W. RNA as scaffold for pyrene excited complexes. *Bioorg. Med. Chem.* **2008**, *16*, 19–26.

(30) Förster, U.; Lommel, K.; Sauter, D.; Grünewald, C.; Engels, J. W.; Wachtveitl, J. 2-(1-Ethynylpyrene)-adenosine as a folding probe for RNA - Pyrene in or out. *ChemBioChem* **2010**, *11*, 664–672.

(31) Förster, U.; Gildenhoff, N.; Grünewald, C.; Engels, J. W.; Wachtveitl, J. Photophysics of 1-ethynylpyrene-modified RNA base adenine. *J. Lumin.* **2009**, *129*, 1454–1458.

(32) Scaringe, S. A.; Wincott, F. E.; Caruthers, M. H. Novel RNA synthesis method using 5′-O-silyl-2′-O-orthoester protecting groups. *J. Am. Chem. Soc.* **1998**, *120*, 11820–11821.

(33) Khan, S. I.; Grinstaff, M. W. Palladium(0)-catalyzed modification of oligonucleotides during automated solid-phase synthesis. *J. Am. Chem. Soc.* **1999**, *121*, 4704–4705.

(34) Robins, M. J.; Uznanski, B. Nucleic-Acid Related-Compounds, Conversions of Adenosine and Guanosine to 2,6-Dichloro, 2-Amino-6-Chloro, and Derived Purine Nucleosides. *Can. J. Chem.* **1981**, *59*, 2601–2607.

(35) Matsuda, A.; Shinozaki, M.; Yamaguchi, T.; Homma, H.; Nomoto, R.; Miyasaka, T.; Watanabe, Y.; Abiru, T. Nucleosides and Nucleotides 0.103. 2-Alkynyladenosines - a Novel Class of Selective Adenosine-A2 Receptor Agonists with Potent Antihypertensive Effects. *J. Med. Chem.* **1992**, *35*, 241–252.

(36) Matsuda, A.; Shinozaki, M.; Suzuki, M.; Watanabe, K.; Miyasaka, T. A Convenient Method for the Selective Acylation of Guanine Nucleosides. *Synthesis* **1986**, 385–386.

(37) Lenz, M. O.; Huber, R.; Schmidt, B.; Gilch, P.; Kalmbach, R.; Engelhard, M.; Wachtveitl, J. First steps of retinal photoisomerization in proteorhodopsin. *Biophys. J.* **2006**, *91*, 255–262.

(38) Kovalenko, S. A.; Dobryakov, A. L.; Ruthmann, J.; Ernsting, N. P. Femtosecond spectroscopy of condensed phases with chirped supercontinuum probing. *Phys. Rev. A* **1999**, *59*, 2369–2384.

(39) Rist, M.; Amann, N.; Wagenknecht, H. A. Preparation of 1-ethynylpyrene-modified DNA via Sonogashira-type solid-phase couplings and characterization of the fluorescence properties for electron-transfer studies. *Eur. J. Org. Chem.* **2003**, 2498–2504.

(40) Seo, Y. J.; Rhee, H.; Joo, T.; Kim, B. H. Self-duplex formation of an A(Py)-substituted oligodeoxyadenylate and its unique fluorescence. *J. Am. Chem. Soc.* **2007**, *129*, 5244–5247.

(41) Hwang, G. T.; Seo, Y. J.; Kim, S. J.; Kim, B. H. Fluorescent oligonucleotide incorporating 5-(1-ethynylpyrenyl)2 ′-deoxyuridine: sequence-specific fluorescence changes upon duplex formation. *Tetrahedron Lett.* **2004**, *45*, 3543–3546.

(42) Mayer, E.; Valis, L.; Wagner, C.; Rist, M.; Amann, N.; Wagenknecht, H. A. 1-ethynylpyrene as a tunable and versatile molecular beacon for DNA. *ChemBioChem* **2004**, *5*, 865–868.

(43) Techert, S.; Schmatz, S.; Wiessner, A.; Staerk, H. Photophysical characteristics of directly linked pyrene-dimethylaniline derivatives. *J. Phys. Chem. A* **2000**, *104*, 5700–5710.

(44) Nakamura, M.; Fukunaga, Y.; Sasa, K.; Ohtoshi, Y.; Kanaori, K.; Hayashi, H.; Nakano, H.; Yamana, K. Pyrene is highly emissive when

attached to the RNA duplex but not to the DNA duplex: the structural basis of this difference. *Nucleic Acids Res.* **2005**, *33*, 5887–5895.

(45) Langenegger, S. M.; Haner, R. Excimer formation by interstrand stacked pyrenes. *Chem. Commun.* **2004**, 2792–2793.

(46) Hwang, G. T.; Seo, Y. J.; Kim, B. H. Pyrene-labeled deoxyuridine and deoxyadenosine: fluorescent discriminating phenomena in their oligonucleotides. *Tetrahedron Lett.* **2005**, *46*, 1475–1477.

(47) Lorenc, M.; Ziolek, M.; Naskrecki, R.; Karolczak, J.; Kubicki, J.; Maciejewski, A. Artifacts in femtosecond transient absorption spectroscopy. *Appl. Phys. B* **2002**, *74*, 19–27.

(48) Tanaka, J. Electronic Spectra of Pyrene Chrysene Azulene Coronene and Tetracene Crystals. *Bull. Chem. Soc. Jpn.* **1965**, *38*, 86–102.

(49) Yoshinaga, T.; Hiratsuka, H.; Tanizaki, Y. Electronic Absorption-Spectra of Pyrene and Hydropyrenes. *Bull. Chem. Soc. Jpn.* **1977**, *50*, 3096–3102.

(50) Neuwahl, F. V. R.; Foggi, P. Direct observation of S-2-S-1 internal conversion in pyrene by femtosecond transient absorption. *Laser Chem.* **1999**, *19*, 375–379.

JP103176Q